

Photosynthesis and calcification in the calcifying algae *Halimeda discoidea* studied with microsensors

D. DE BEER¹ & A. W. D. LARKUM²

¹Max-Planck-Institute for Marine Microbiology, D-28359 Bremen, Germany and ²School of Biological Sciences, University of Sydney, Sydney, Australia

ABSTRACT

With microsensors, we measured the steady-state micro-profiles of O₂, pH and Ca²⁺ on the topside of young segments of *Halimeda discoidea*, as well as the surface dynamics upon light–dark shifts. The effect of several inhibitors was studied. The steady-state measurements showed that under high light intensity, calcium and protons were taken up, while O₂ was produced. In the dark, O₂ was consumed, the pH decreased to below seawater level and Ca²⁺ uptake was reduced to 50%. At low light intensity (12 μmol photons m⁻² s⁻¹), Ca²⁺ efflux was observed. Upon light–dark shifts, a complicated pattern of both the pH and calcium surface dynamics was observed. Illumination caused an initial pH decrease, followed by a gradual pH increase: this indicated that the surface pH of *H. discoidea* is determined by more than one light-induced process. When photosynthesis was inhibited by dichlorophenyl dimethyl urea (DCMU), a strong acidification was observed upon illumination. The nature and physiological function of this putative pump is not known. The calcium dynamics followed all pH dynamics closely, both in the presence and absence of DCMU. The Ca-channel blockers verapamil and nifedipine had no effect on the Ca²⁺ dynamics and steady-state profiles. Thus, in *H. discoidea*, calcification is not regulated by the alga, but is a consequence of pH increase during photosynthesis. Acetazolamide had no effect on photosynthesis, whereas ethoxzolamide inhibited photosynthesis at higher light intensities. Therefore, all carbonic anhydrase activity is intracellular. Carbonic anhydrase is required to alleviate the CO₂ limitation. Calcification cannot supply sufficient protons and CO₂ to sustain photosynthesis.

Key-words: Calcium; dynamics; fluxes; oxygen; pH.

INTRODUCTION

Calcification is a common phenomenon in aquatic photosynthetic communities, particularly in marine environments (Borowitzka 1984). Reef-building corals are the most spectacular examples; however, micro- and macroalgae are also important calcifiers, even in coral reef systems (Gattuso *et al.* 1997; Larkum 1999). Biogenic calcification is closely coupled to photosynthesis, because of the shift in the car-

bonate system by CO₂ uptake and the concomitant pH increase, which enhances the calcium carbonate precipitation (Borowitzka 1984; McConnaughey 1987). As the calcification reaction produces H⁺ and CO₂, it decreases the changes in pH and CO₂ concentration induced by photosynthesis. It is hypothesized that in the green alga *Chara* (McConnaughey & Falk 1991; McConnaughey 1991) and in foraminifera (Erez 1983), calcification enhances photosynthesis by reducing alkalinity and increasing the availability of CO₂.

Extensive studies have been performed on calcification in *Halimeda tuna* and *Halimeda cylindrica* (Borowitzka & Larkum 1976a, b; c, d). In *Halimeda*, aragonite crystals are deposited in the intercellular spaces (Borowitzka & Larkum 1976a), separated from the seawater by a layer of appressed cells (utricles), in which the photosynthetic activity is concentrated. Solutes, exchanging with seawater, have to pass through the utricles layer as well as the mass boundary layer adjacent to the tissue. It was hypothesized that during photosynthesis, the diffusion barrier allows the development of a microenvironment with a high pH, suitable for aragonite precipitation (Borowitzka & Larkum 1976b, c, d). Thus, in *Halimeda*, calcification is thought to be regulated by the morphology of the algae: the tissue does not have a regulatory influence except through the uptake of CO₂ by photosynthesis and maybe as a nucleation site for calcification (Borowitzka 1989). Recently, we reported on a microsensor study on corals, showing that calcium uptake at the tissue was influenced directly by photosynthesis (de Beer *et al.* 2000). We concluded that this might be an active regulatory mechanism to fine-tune the pH regulation within the tissue of corals. Here, we used microsensor techniques to explore the relationship between photosynthesis and calcification in the calcifying alga *Halimeda discoidea*.

MATERIALS AND METHODS

Sampling and incubations

Halimeda discoidea specimens were collected in August 1999 on the inner border of the Heron Island lagoon (Australia). The seawater temperature was approximately 18 °C. After collection, samples were stored in a tank on shore and flushed continuously with fresh seawater. Measurements were performed within 3 d of collection.

For laboratory experiments, specimens consisting of three to four segments were placed in a flow cell, through

Correspondence: Dirk de Beer. E-mail: dbeer@mpi-bremen.de

which seawater was pumped from a continuously aerated recirculation tank. The recirculation tank contained 120 dm³ of seawater that was refreshed daily. The flow rate around the specimen was approximately 5 cm s⁻¹, judged from the velocity of suspended particles. The temperature during experiments was 20 °C, which is close to the ambient seawater temperature. Microsensor measurements were performed during daytime to avoid the effects of diel migration of the chloroplasts (Drew & Abel 1990). The light source was a fibre optic halogen lamp (Schott KL1500 or Schott KL2500; Schott, Mainz, Germany). Incident light intensity was quantified as down-welling scalar irradiance with a Biospherical Instruments meter (QSL-100; San Diego, CA, USA). Most experiments were performed with the Schott KL1500, allowing a maximum light intensity of 200 $\mu\text{mol photons m}^{-2} \text{s}^{-1}$ during microsensor measurements. The effect of the quality of the light on pH dynamics was investigated by using LP 530 and LP 630 filters placed in the light path of the Schott KL2500. The total light intensity during these measurements was maintained at 100 $\mu\text{mol photons m}^{-2} \text{s}^{-1}$.

Microsensors

Liquid membrane type Ca²⁺ and pH microsensors were prepared and calibrated as described previously (de Beer *et al.* 1997, 2000). The absence of tissue surface-potentials, which could add to the signals of the pH and Ca²⁺ microsensors, was checked carefully with blank sensors (microcapillaries filled with 3 M KCl adjusted to pH 2.5). Fast-responding O₂ microsensors were prepared as described previously (Revsbech 1989). All microsensors had response times (t_{90}) of less than 1 s.

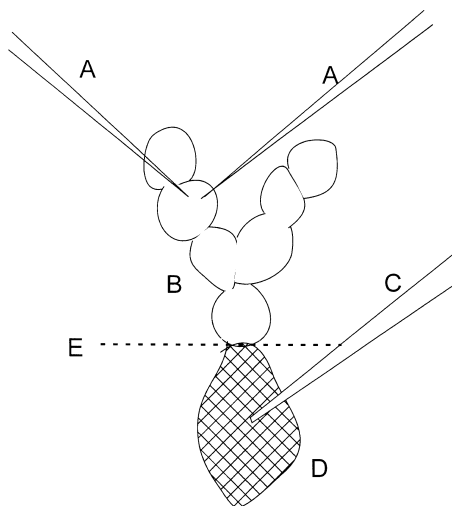


Figure 1. Sketch of the microsensor measurements. In most experiments, two microsensors (A) were positioned simultaneously at the thallus (B) surface. In one experiment, a thicker pH sensor (C) was positioned in the calcified rhizoid zone (D), while one microsensor (A) was positioned at the thallus surface. The sediment surface (E) is indicated by the dashed line.

The positions of the sensors during measurements are shown in Fig. 1. As penetration into the algae caused artifacts, microsensor measurements were restricted to the thallus surface or the boundary layer. A shutter (Vincent Associates, Rochester, NY, USA) was used for rapid darkening. The concentration dynamics at the thallus surface were recorded simultaneously with two different microsensors positioned at the thallus surface, with their measuring tips less than 100 μm apart. The measurements were carried out on the second segment from the top.

Measurements of the pH in the rhizoid zone were carried out with liquid membrane type sensors of 1 mm tip diameter. The tip of a silanized glass capillary was sealed with an approximately 3-mm-thick membrane cocktail (as used for the pH microsensors) and left overnight to solidify. Subsequently, the shaft was filled with the electrolyte. The examined specimen had an egg-shaped calcified rhizoid zone of approximately 4 cm depth and a maximum diameter of 3 cm. The sensor was positioned close to the middle so that the tip was approximately 2 cm below the sediment surface. A pH microsensor was positioned at the thallus surface of the same specimen. The pH at the thallus surface and in the rhizoid zone was followed during three daily cycles (approximately 12 h light : 12 h dark). Only the thallus was illuminated.

Gross photosynthetic rates were determined with O₂ microsensors by the light–dark shift method (Revsbech & Jørgensen 1983; Glud, Ramsing & Revsbech 1992; Kühl *et al.* 1996), using the initial rate (< 2 s) of O₂ depletion after darkening. Profiles were measured by positioning the microsensors using a motorized micromanipulator. The sensors were manipulated at an angle of 20° relative to the incident light. The thallus surface was the reference point (depth = 0), determined with a dissection microscope. Negative depths indicate positions above the surface.

Interfacial fluxes (J) were calculated from the concentration profiles using Fick's first law:

$$J = D \times (dc/dx),$$

where D is the diffusion coefficient and dc/dx is the interfacial concentration gradient, i.e. the concentration gradient in the mass boundary layer directly adjacent to the tissue.

Pulse amplitude modulation

Chlorophyll fluorescence quantum yield, recorded by a Teaching-PAM (PAM-200; Walz GmbH, Effeltrich Germany) equipped with a glass fibre lead, was used in addition to the microsensor measurements of gross photosynthesis to determine whether dichlorophenyl dimethyl urea (DCMU) had been effective. The glass fibre was positioned approximately 5 mm from the thallus surface. Light intensities ranged from 10 to 1200 $\mu\text{mol photons m}^{-2} \text{s}^{-1}$.

Diffusion coefficients

The diffusion coefficients of O₂ and Ca²⁺ in seawater at 20 °C are literature values corrected for temperature and

type of counter ion (Broecker & Peng 1974; Li & Gregory 1974): the diffusion coefficient of O_2 is $1.97 \times 10^{-9} \text{ m}^2 \text{ s}^{-1}$; the self-diffusion coefficient of Ca^{2+} is $0.71 \times 10^{-9} \text{ m}^2 \text{ s}^{-1}$; the diffusion coefficient of Ca^{2+} (with HCO_3^- as counter ion) was calculated to be $0.86 \times 10^{-9} \text{ m}^2 \text{ s}^{-1}$.

Inhibitors

Ethoxzolamide, an inhibitor of carbonic anhydrase that can penetrate into cells, was dissolved in dimethyl sulphoxide (DMSO) and added to a final concentration of 0.3 mol m^{-3} (Tambutte *et al.* 1995). The final DMSO concentration was 0.1%, which had no effect on surface Ca^{2+} and O_2 concentrations and gross photosynthesis. Acetazolamide, an inhibitor of carbonic anhydrase that cannot penetrate into cells, was dissolved in distilled water and added to a final concentration of 1 mol m^{-3} (Tambutte *et al.* 1995). DCMU, a strong inhibitor of photosystem II, was dissolved in ethanol and added to final concentrations of 0.5 and 2.5 mmol m^{-3} (Ip & Krisnaveni 1991). The final ethanol concentrations did not exceed 0.01%, which had no effect on surface pH values, Ca^{2+} and O_2 concentrations in a blank experiment. Verapamil, a Ca^{2+} channel blocker (N-type) was dissolved in DMSO and added to a final concentration of 0.1 or 0.5 mmol m^{-3} (Marshall 1996). The final DMSO concentrations did not exceed 0.01%. Nifedipine, an L-type Ca^{2+} channel blocker, was dissolved in DMSO and added to a final concentration of 0.1 mol m^{-3} (Reid & Smith 1992; Stento *et al.* 2000). For inhibitor experiments, a recycle tank of 1 dm^3 was used to reduce the amount of inhibitors. In a blank experiment, no effect on photosynthesis was observed by reducing the recycle to 1 dm^3 . The effect of all inhibitors was monitored for at least 3 h. After each inhibitor experiment, the flow cell was cleaned thoroughly with water, detergent and ethanol and finally rinsed with water. Fresh specimens and fresh seawater were used for each inhibitor experiment.

RESULTS

Penetration of the microsensors into the thallus appeared to be impossible without damaging the segment and the induction of abnormal signals. Upon penetration, the tissue burst locally (approximately $10 \mu\text{m}$ around the sensor tip) and a small amount of viscous slime was extruded in a wound reaction. This resulted in a sudden decrease of the pH value (from approximately pH 8 to pH 4–5) and the Ca^{2+} concentration (from approximately 9 to $1\text{--}3 \text{ mol m}^{-3}$). The signals recovered to normal values within 10 min. The effect on the O_2 signals was rather small. All reported measurements were limited to the thallus surface and adjacent mass boundary layer. No potentials could be detected at the tissue surface with blank sensors.

Under the flow conditions imposed a hypothetical mass boundary layer, defined by the intercept of the interfacial gradient with the concentration in the seawater, was observed of approximately $500 \mu\text{m}$, as inferred from Ca^{2+}

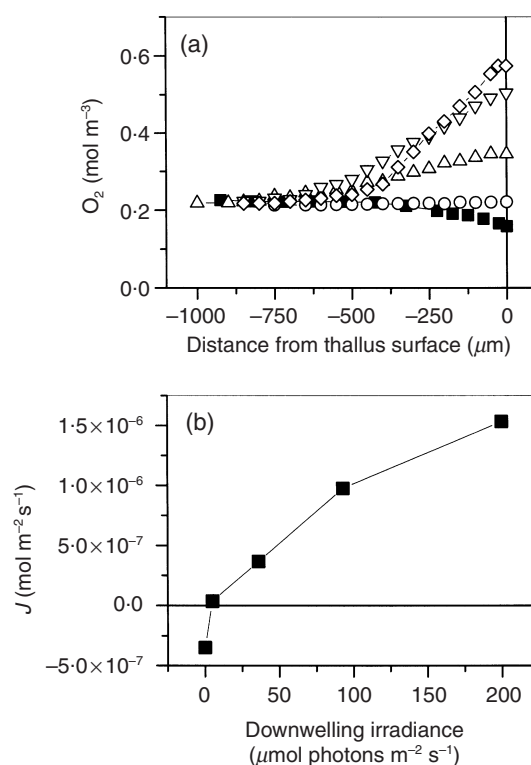


Figure 2. (a) Oxygen profiles measured at light intensities of 0 (■), 12 (●), 36 (△), 93 (▽) and $200 (\diamond) \mu\text{mol photons m}^{-2} \text{ s}^{-1}$. (b) Interfacial fluxes calculated from these profiles. The profile measurements were carried out in the mass boundary layer; the thallus surface is at a depth of $0 \mu\text{m}$. The fluxes are calculated from the concentration gradient at the thallus surface using Fick's first law of diffusion.

and O_2 steady-state profiles. The steady-state profiles of O_2 , pH and Ca^{2+} (Figs 2a & 3a) were, as expected, strongly influenced by light. In the dark, oxygen was consumed by respiration in the tissue, leading to a small oxygen decrease at the surface. With increasing light intensities, the surface concentration increased up to approximately 2.5 times the seawater concentration (at $200 \mu\text{mol photons m}^{-2} \text{ s}^{-1}$). The surface pH in the dark was approximately 8.0, slightly below that of seawater, whereas in the light the pH increased to a value of 8.8 (Fig. 3a). In the dark, the Ca^{2+} concentration at the thallus surface was 8.8 mol m^{-3} (0.2 mol m^{-3} below that of seawater), light decreased the surface concentration further to 8.6. As the Ca^{2+} surface concentration was below the seawater concentration, calcium uptake (and thus calcification) occurred in the dark. In the light, the surface concentration decreased further, showing that calcification was strongly stimulated by light. As calculated from the gradients at the surface, *H. discoidea* took up O_2 ($3.5 \times 10^{-7} \text{ mol m}^{-2} \text{ s}^{-1}$) and Ca^{2+} ($3.9 \times 10^{-7} \text{ mol m}^{-2} \text{ s}^{-1}$) in the dark. During illumination, O_2 production is approximately twice the Ca^{2+} uptake (15.3×10^{-7} and $8.8 \times 10^{-7} \text{ mol m}^{-2} \text{ s}^{-1}$, respectively).

Photosynthesis as a function of light intensity was determined by fast O microsensors. Gross photosynthesis was

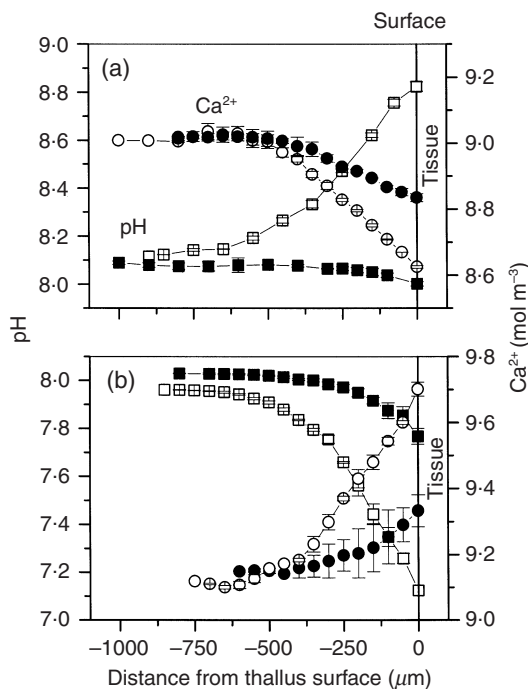


Figure 3. (a) Calcium (●, ○) and pH (■, □) profiles in the mass boundary layer of untreated *H. discoidea* segments in the dark (filled symbols) and light (open symbols). (b) The same type of profiles above *H. discoidea* treated with DCMU. The measurements were carried out in the mass boundary layer; the thallus surface is at a depth of 0 μm .

determined with the light–dark shift microsensor technique and the net photosynthesis was determined from the interfacial gradients. The gross photosynthesis increased up to the highest applied light intensity of 200 $\mu\text{mol photons m}^{-2} \text{s}^{-1}$ (Fig. 4). The net oxygen production increased, but did not level off at the same light intensity (Fig. 2b). From these measurements, it is clear that no photoinhibition occurs at a light intensity of 200 $\mu\text{mol photons m}^{-2} \text{s}^{-1}$.

Furthermore, the response of surface concentrations to illumination and darkening in periods of 15 min to 1 h were measured. All parameters showed a significant response to changes in light conditions. O_2 always responded instantly in one direction, a decrease upon darkening and an increase upon illumination (Fig. 5). Ca^{2+} and pH showed a more complicated pattern, depending on the light intensities (Figs 5 & 6). Upon illumination with 200 $\mu\text{mol photons m}^{-2} \text{s}^{-1}$, O_2 increased instantly, whereas Ca^{2+} and pH remained more or less constant for 20–30 s, although small fluctuations were visible. After this delay, a rapid increase in pH and decrease in Ca^{2+} surface concentration was observed. At lower light intensities (36 and 93 $\mu\text{mol photons m}^{-2} \text{s}^{-1}$) a complicated pattern in pH and Ca^{2+} dynamics was visible. Initially the pH increased, which is the expected response to photosynthesis. This was followed by a decrease, which was again followed by an increase. The Ca^{2+} surface concentration showed a similar pattern. Upon darkening, the pH decreased sharply, followed by a gradual

increase to a value close to that of seawater. Illuminating with 12 $\mu\text{mol photons m}^{-2} \text{s}^{-1}$ caused an initial pH increase, followed by a decrease to a stable level below the seawater value. A light intensity of 5 $\mu\text{mol photons m}^{-2} \text{s}^{-1}$ did not have significant effects. Thus, illumination with low light results in a pH decrease at the thallus surface although net photosynthesis occurs. The steady-state pH value at 12 $\mu\text{mol photons m}^{-2} \text{s}^{-1}$ was 7.5, or approximately 0.5 units below that in the absence of light. At this low light intensity, the steady-state Ca^{2+} concentration was almost 10 mol m^{-3} or approximately 0.5 mol m^{-3} higher than that in the dark. Therefore, both in high light and in darkness, Ca^{2+} uptake occurred, but at low light intensities Ca^{2+} efflux was observed. These patterns were reproducible, and were observed on different individuals.

The effect of light quality on the complex pH dynamics was investigated by the use of LP 530 and LP 630 light filters. These filters effectively removed all light of wavelengths shorter than 530 nm and 630 nm, respectively. At equal light intensities, the same pH dynamics were observed, regardless of the filters used (data not shown). Thus the complex pattern of pH dynamics upon illumination (see Figs 4 & 5) is independent of the light quality.

In the presence of DCMU, which inhibits photosystem II and thereby non-cyclic photosynthetic electron transport, no oxygen dynamics were observed and with PAM the absence of photosynthetic activity was confirmed. Surprisingly, pH and Ca^{2+} dynamics did not stop, but showed an inverse pattern as in the absence of DCMU (Fig. 7): upon illumination, the pH decreased and the Ca^{2+} concentration increased; upon darkening, the reverse occurred. The pH and Ca^{2+} dynamics increased with the light intensity and no saturation in amplitude or response rates was observed at 200 $\mu\text{mol photons m}^{-2} \text{s}^{-1}$. After the addition of DCMU, the Ca^{2+} surface concentrations were higher than the surrounding seawater (Fig. 2b). The efflux, calculated from the interfacial profiles, was $0.63 \times 10^{-6} \text{ mol m}^{-2} \text{s}^{-1}$ in the dark; light enhanced the efflux to $1.2 \times 10^{-6} \text{ mol m}^{-2} \text{s}^{-1}$.

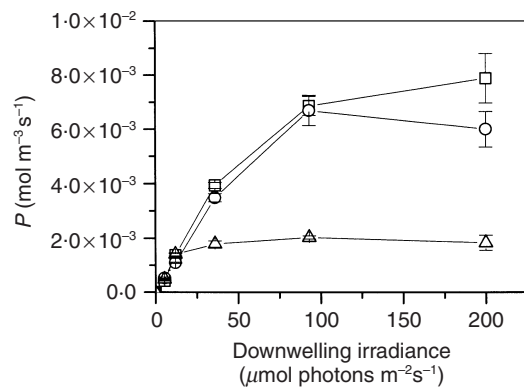


Figure 4. Gross photosynthesis rates of untreated *H. discoidea* segments (□), after acetazolamide treatment (○) and after treatment with ethoxzolamide (△). These compounds inhibit carbonic anhydrase; only ethoxzolamide can penetrate cells.

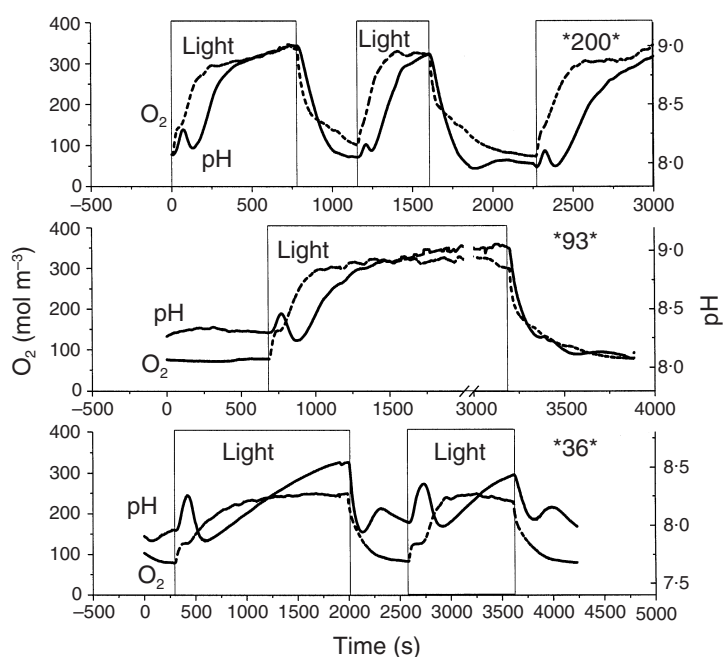


Figure 5. Oxygen (dashed line) and pH (solid line) dynamics upon illumination and darkening at the surface of *H. discoidea*. The numbers between asterisks indicate the light intensities in $\mu\text{mol photons m}^{-2} \text{s}^{-1}$.

Long-term pH dynamics were recorded simultaneously at the thallus surface and in the rhizoid zone. This was carried out because we observed that upon planting thallus fragments in sediment, extensive calcification seemed to occur in the developing rhizoid zone, leading to a porous clump. The pH in the rhizoid zone varied between 7.5 and 7.8. Upon illumination of the thallus, the pH decreased temporarily, followed by a return to the original value (Fig. 8). Upon darkening, no pH change was observed. The pH fluctuations in the rhizoid zone were much slower than those at the thallus surface. The amplitude of the pH change and the time needed for return to the initial value was dependent on the light intensity. Upon illumination with $200 \mu\text{mol photons m}^{-2} \text{s}^{-1}$, the decrease was 0.1–0.2 pH units, and lasted approximately 1 h. Upon illumination with 750 or $1500 \mu\text{mol photons m}^{-2} \text{s}^{-1}$, the decrease was 0.3 pH units and lasted 2–3 h.

The addition of verapamil did not affect the photosynthesis rate or the Ca^{2+} dynamics (data not shown), even at a concentration of 1 mmol m^{-3} , which is 10 times the recommended concentration for coral studies (Marshall 1996). Nifedipine (0.1 mol m^{-3}) changed the pH and Ca^{2+} dynamics to some extent, although the complex pattern was still present (Fig. 9). The photosynthesis rates were unchanged by nifedipine under all light intensities, i.e. the PI curve did not change (data not shown).

Acetazolamide did not affect gross photosynthesis (Fig. 4) or the oxygen efflux. The addition of ethoxzolamide decreased photosynthesis above a light intensity of $12 \mu\text{mol photons m}^{-2} \text{s}^{-1}$ to approximately 25% of the control rate (Fig. 4). The Ca^{2+} dynamics were not influenced by acetazolamide, whereas ethoxzolamide reduced the amplitude from 0.7 mol m^{-3} to less than 0.1 mol m^{-3} (data not shown).

DISCUSSION

For the precise determination of light respiration and net photosynthesis O_2 profiles inside the thallus are needed (Kühl *et al.* 1996). Furthermore, pH and Ca^{2+} measurements at the site of calcification (the intertricular space) would give unambiguous information on the calcification mechanism. However, penetration of the microsensors into the thallus without disturbance was impossible. The extrusion of viscous liquid upon penetration of a microsensor in the thallus is a typical wounding reaction, leading to the formation of a plug. The low pH of the viscous liquid may originate from a defence mechanism of the algae against predation (Hay, Kappel & Fenical 1994; Loban & Harrison 1997). This behaviour limits the microsensor research to the surface and the boundary layer. In general, our results confirm conclusions made in previous experiments based on a different experimental approach (Borowitzka & Larkum 1976b, c, d) and extend them significantly.

The pH effects can only be explained partially by the influence of photosynthesis, respiration and calcification on the carbonate system. CO_2 uptake for photosynthesis leads to an increase in pH, whereas CO_2 and H^+ release by respiration and calcification leads to a pH decrease. Thus both dark respiration and dark calcification are responsible for the pH decrease at the thallus surface, whereas in the light CO_2 uptake for photosynthesis must be higher than the combined CO_2 release by calcification and respiration to reach values above seawater. The precise synchronization of the Ca^{2+} and pH dynamics is consistent with the hypothesis that the chemical environment (in the intertricular spaces) is the major determinant of CaCO_3 precipitation: the degree of over-saturation of Ca^{2+} and CO_3^{2-} ions is determined by the local pH. No evidence for regulation of

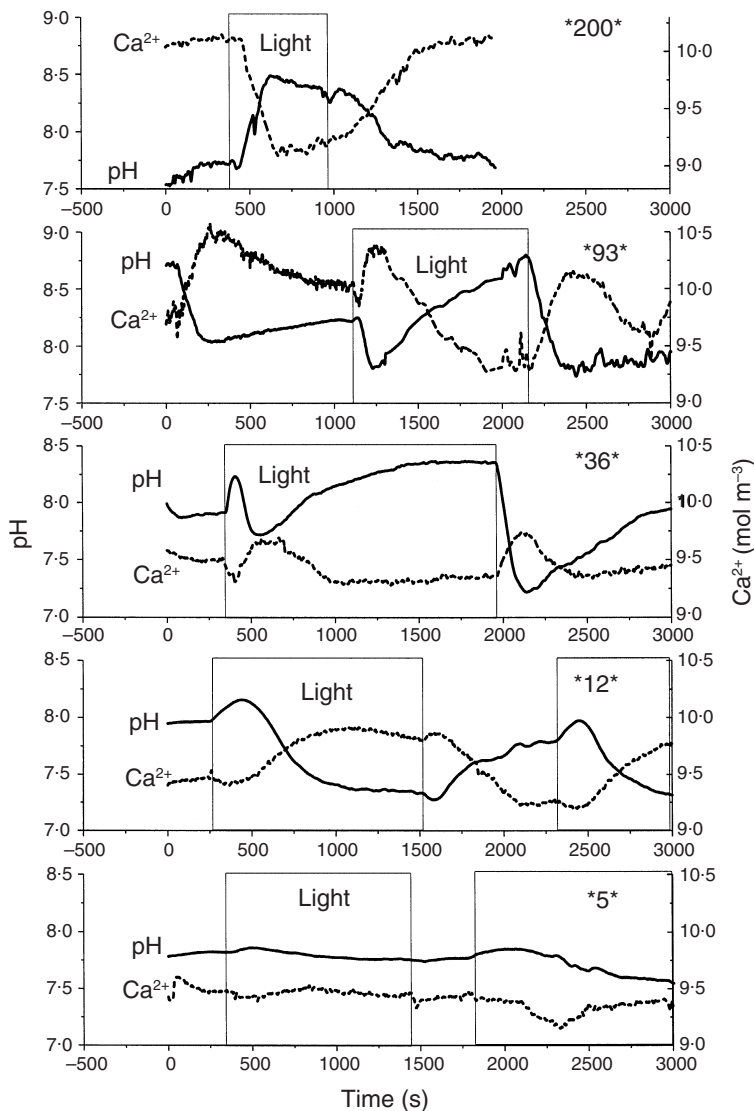


Figure 6. Ca^{2+} (dashed line) and pH (solid line) dynamics upon illumination and darkening at the surface of *H. discoidea*. The numbers between asterisks indicate the light intensities in $\mu\text{mol photons m}^{-2} \text{s}^{-1}$.

Ca^{2+} uptake by the algae was found, as previously reported for corals (de Beer *et al.* 2000). In most calcifying algae, calcification occurs extra-cellularly, in direct contact with the surrounding water, whereas in corals the site of calcification is shielded from the seawater by the coral tissue. The latter situation allows direct control over the calcium transport and thus over the calcification process. In *Halimeda*, calcification occurs in the intertricular spaces that have a diffusive connection via cell walls with seawater (Borowitzka & Larkum 1976c). We tested both verapamil, a N-type Ca^{2+} channel blocker, and nifedipine, an often-used L-type Ca^{2+} channel blocker that was shown to be effective in *Chara* (Reid & Smith 1992; Stento *et al.* 2000). Indeed, neither Ca^{2+} channel blockers had any effect on Ca^{2+} dynamics, indicating that trans-membrane Ca^{2+} transport does not play a role in the calcification.

In light the Ca^{2+} influx was approximately 50% of the O_2 efflux. Previous studies on *Halimeda cylindrica* showed calcification to be less than 25% of the photosynthetic CO_2

binding (Borowitzka & Larkum 1976b). Calcification in *Halimeda tuna* was approximately 40% of the net photosynthesis rate in all segments. This corresponds to our findings, assuming O_2 production and CO_2 fixation are close to stoichiometric unity.

An interesting finding was that oxygenic photosynthesis is not the only light-induced factor that influences the pH at the segment surface. The complicated patterns of pH dynamics can only be explained by the presence of two light-dependent processes influencing the pH in opposite directions. In addition to oxygenic photosynthesis, which is accompanied by proton consumption, a proton-generating process is triggered by light. Indeed, when non-cyclic photosynthetic electron transport was inhibited by DCMU, pH dynamics did not stop, but continued in the opposite direction. Calcification can be ruled out as a proton-generating process, as the pH decrease was accompanied by Ca^{2+} increase, i.e. calcium carbonate dissolution. It is obvious from the experiments with DCMU that this putative proton

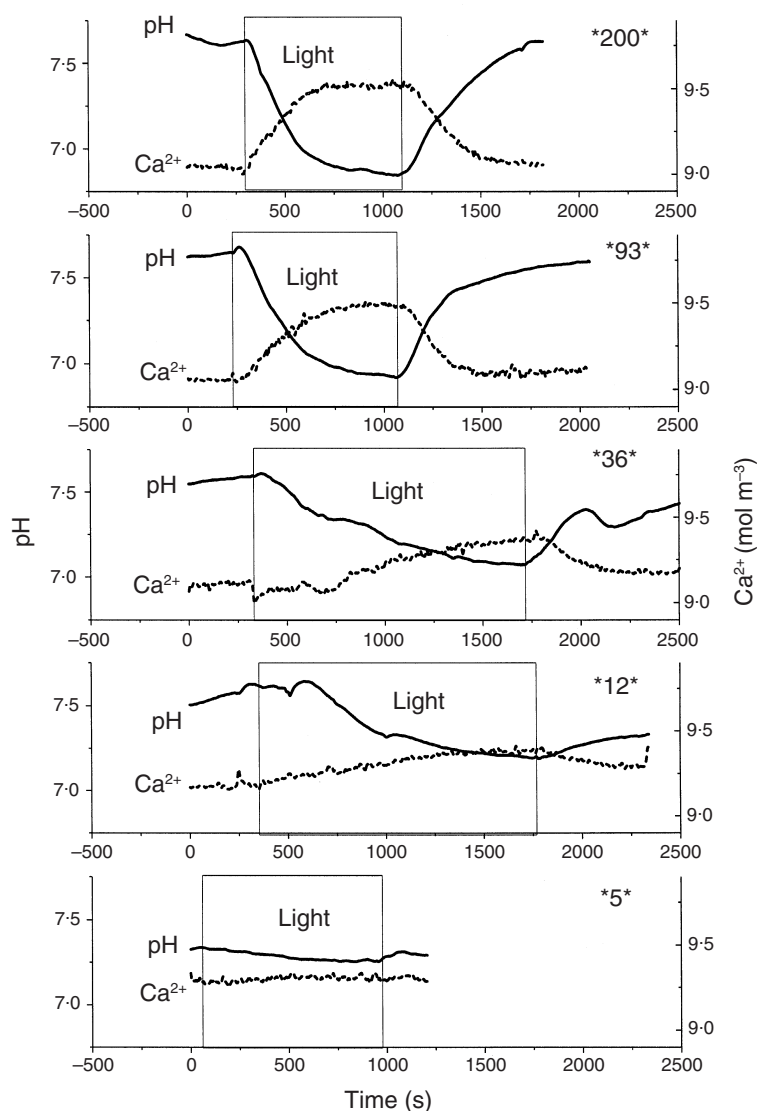


Figure 7. Ca^{2+} and pH dynamics upon illumination and darkening at the surface of *H. discoidea*. In this experiment, photosynthesis was inhibited with DCMU. The numbers between asterisks indicate the light intensities in $\mu\text{mol photons m}^{-2} \text{s}^{-1}$.

pump is not tightly coupled to non-cyclic photosynthetic electron transport. The occurrence of light-induced proton pumping, independent of non-cyclic photosynthetic electron transport has not yet been reported for algae, although it was indirectly implicated in previous evidence (Borowitzka & Larkum 1976d). In guard cells of stomata from higher plants, an intracellular light-induced pH shift is brought about by weak blue light (Assmann, Simoncini & Schroeder 1985; Shimazaki, Iino & Zeiger 1986). However, such a dependence on the wavelength was not observed in our study, and in addition light with a wavelength of more than 630 nm induced the proton efflux. The pump could be an ATP-dependent process, where ATP is formed by respiration or by cyclic photosynthetic electron transport by photosystem I (Raven, Evans & Korb 1999). Another possible explanation is that a proton exchange system (e.g. H^+-K^+) is inhibited by light. The function of this light-driven or light-activated proton pump is puzzling and so is its consequence for the intracellular chemistry. The cytoplasmic pH

ranges from 7 to 7.5, which needs to be maintained actively during photosynthesis. If the outwardly directed proton pump is regulated by the internal pH, i.e. it is inhibited by high internal pH, it would contribute to the intracellular homeostasis. However, we showed that at low light intensities, oxygenic photosynthesis is accompanied by a lowering of the surface pH to below the value of seawater. Whatever the mechanism is for the light-induced pH decrease at the surface, either reduced proton uptake or increased proton efflux, it must result in a pH increase in the cytoplasm. Additionally, the cytoplasmic pH would increase during oxygenic photosynthesis due to CO_2 fixation. Possibly, *H. discoidea* exhibits a heterogeneous pattern of proton uptake at one location and efflux at another, similar to *Chara* (McConnaughey 1991). If present in *H. discoidea*, heterogeneously distributed proton exchange patterns will control to some extent the site of calcification, most effectively at low light intensities. Although in complete darkness Ca^{2+} uptake occurred, at low light intensities

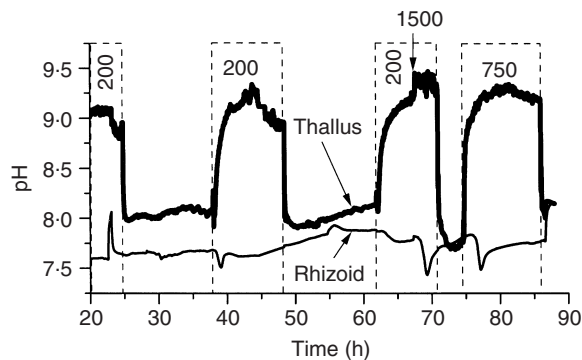


Figure 8. The pH dynamics measured in the rhizoid zone (thin line) and at the thallus surface (thick line) of *Halimeda* during long cycles of illumination and darkness. The numbers in the blocks indicate the light intensities in $\mu\text{mol photons m}^{-2} \text{s}^{-1}$.

Ca^{2+} efflux from the thallus, and thus decalcification, was observed. This might prevent or reduce calcification of *H. discoidea* at such low light intensities, possibly as an adaptation to low-light *in situ* conditions of typically $20 \mu\text{mol photons m}^{-2} \text{s}^{-1}$ (Jensen *et al.* 1985). In a first attempt to detect such heterogeneous proton pumps we measured the pH in the rhizoid zone. It is clear that we could not demonstrate that the root zone acts as a source for protons, as acidification occurred upon illumination. Possibly, this is caused by fermentation or oxidation of photosynthates formed in the light and excreted by the rhizoids, although this cannot explain the transient character of the acidification. Alternatively, oxygen produced in the thallus may be transported downwards and induce oxidation of the sulphide pool formed during darkness. Further research to elucidate these questions is planned.

A further observation is the stronger dark acidification in the presence of DCMU, which led to decalcification in the dark (compare Fig. 2a and 2b). During DCMU incubation, the O_2 surface concentration gradually decreased from approximately 0.16 to 0.13 mol m^{-3} , thus the increase of dark respiration seems to be a side-effect of this inhibitor. This increased respiration caused by DCMU induced the pH decrease. The results again show that calcium uptake or release are tightly coupled to the pH.

Inhibition of carbonic anhydrase strongly reduced the gross photosynthesis, particularly at higher light intensities. As only ethoxzolamide, which can penetrate cell membranes, is effective, the carbonic anhydrase seems to be located only inside the cells. This has been reported previously in other marine algae (Huertas *et al.* 2000). However, it is contrary to previous findings on *Halimeda tuna*, in which net photosynthesis was strongly inhibited by acetazolamide (the generic name Diamox was used), which cannot penetrate cell membranes (Borowitzka & Larkum 1976d). We cannot explain this discrepancy. The high net photosynthesis rates of *H. discoidea* can only be sustained by HCO_3^- , the role of carbonic anhydrase is as the catalysis of conversion of HCO_3^- to CO_2 . Inhibition of photosynthe-

sis by ethoxzolamide is most prominent at higher light intensities, which is consistent with the view that under these conditions C_i (HCO_3^- and CO_2) transport limits photosynthesis. These results emphasize the role of carbonic anhydrase in the CO_2 supply to Rubisco during high rates of photosynthesis. Obviously, calcification cannot supply sufficient CO_2 to sustain photosynthesis, demonstrating that calcification is rather a consequence than a booster of photosynthesis.

CONCLUSIONS

Calcium dynamics are largely determined by pH, as opposed to corals where Ca^{2+} uptake is light-triggered. This is consistent with the hypothesis that calcium precipitation is regulated by physical factors: the local pH at the calcification site and over-saturation of calcium carbonate in the seawater. Photosynthesis, respiration and a light-driven proton pump determine the local pH. A strong light-driven or light-triggered proton pump is present in the algae-exporting protons. As a consequence of this, the cytoplasm will increase its pH, even in the absence of photosynthetic CO_2 fixation. As the pump is also active during non-cyclic photosynthetic electron transport, it will enhance the internal pH even further: therefore, we speculate on a heterogeneous distribution of proton uptake and release. The function of this putative pump is unknown, but it might have a role in the regulation of calcification. The calcification of *H. discoidea* is directly coupled to the local pH, thus

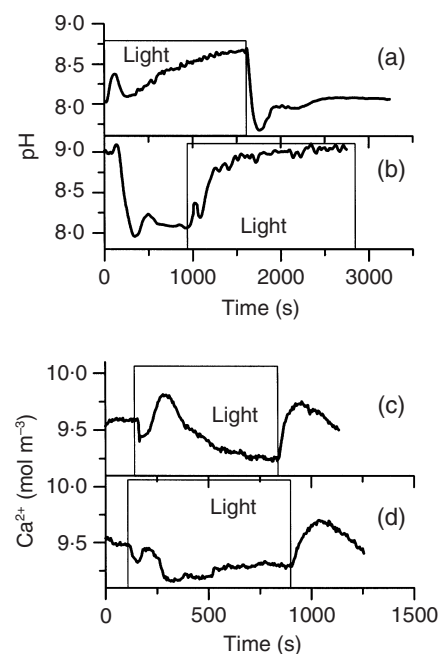


Figure 9. Effect of nifedipine on the pH and Ca^{2+} dynamics in response to $100 \mu\text{mol photons m}^{-2} \text{s}^{-1}$. (a) and (c) are the blank and (b) and (d) represent the nifedipine-treated specimens.

it is to be expected that acidification of seawater will decrease the calcification.

ACKNOWLEDGMENTS

We thank Gaby Eickert, Anja Eggers and Vera Hubner for the construction of microsensors and Anja Eggers for technical assistance during the microsensor measurements. We thank the staff from the Heron Island Research Station for their hospitality, the technical support and the help with the logistic problems.

REFERENCES

- Assmann S.M., Simoncini L. & Schroeder J.I. (1985) Blue light activates electrogenic ion pumping in guard cell protoplasts of *Vicia faba*. *Nature* **318**, 285–287.
- de Beer D., Kühl M., Stambler N. & Vaki L. (2000) A microsensor study of light enhanced Ca^{2+} uptake and photosynthesis in the reef-building hermatypic coral *Favia* sp. *Marine Ecology Progress Series* **194**, 75–85.
- de Beer D., Schramm A., Santegoeds C.M. & Kühl M. (1997) A nitrite microsensor for profiling environmental biofilms. *Applied and Environmental Microbiology* **63**, 973–977.
- Borowitzka M.A. (1984) Calcification in aquatic plants. *Plant, Cell and Environment* **7**, 457–466.
- Borowitzka M.A. (1989) Carbonate calcification in algae – initiation and control. In *Biominalization* (eds S. Mann, J. Webb & R.J.P. Williams), pp. 63–94. VHC Verlag, Berlin.
- Borowitzka M.A. & Larkum A.W.D. (1976a) Calcification in the green algae *Halimeda*. I. An ultrastructure study of thallus development. *Journal of Phycology* **13**, 6–16.
- Borowitzka M.A. & Larkum A.W.D. (1976b) Calcification in the green algae *Halimeda*. II. The exchange of ^{45}Ca and the occurrence of age gradients in calcification and photosynthesis. *Journal of Experimental Botany* **27**, 864–878.
- Borowitzka M.A. & Larkum A.W.D. (1976c) Calcification in the green algae *Halimeda*. III. The sources of inorganic carbon for photosynthesis and calcification and a model of the mechanism of calcification. *Journal of Experimental Botany* **27**, 879–893.
- Borowitzka M.A. & Larkum A.W.D. (1976d) Calcification in the green algae *Halimeda*. IV. The action of metabolic inhibitors on photosynthesis and calcification. *Journal of Experimental Botany* **27**, 894–907.
- Broecker W.S. & Peng T.-H. (1974) Gas exchange rates between air and sea. *Tellus* **26**, 21–35.
- Drew E.A. & Abel K.M. (1990) Studies on *Halimeda* III. A daily cycle of chloroplast migration within segments. *Botanica Marina* **33**, 31–46.
- Erez J. (1983) Calcification rates, photosynthesis and light in planktonic foraminifera. In *Biominalization and Biological Metal Accumulation* (eds P. Westbroek & E.W. de Jong), pp. 307–312. D. Reidel Publishing Co., Dordrecht, The Netherlands.
- Gattuso J.P., Payri C.E., Pichon M., Delesalle B. & Frankignoulle M. (1997) Primary production, calcification, and air-sea CO_2 fluxes of a macroalgal-dominated coral reef community (Moorea, French Polynesia). *Journal of Phycology* **33**, 729–738.
- Glud R.N., Ramsing B. & Revsbech N.P. (1992) Photosynthesis and photosynthesis-coupled respiration in natural biofilms quantified with oxygen microsensors. *Journal of Phycology* **28**, 51–60.
- Hay M.E., Kappel Q.E. & Fenical W. (1994) Synergisms in plant defenses against herbivores: interactions of chemistry, calcification and plant quality. *Ecology* **75**, 1714–1726.
- Huertas I.E., Colman B., Espie G.S. & Lubian L.M. (2000) Active transport of CO_2 by three species of marine microalgae. *Journal of Phycology* **36**, 314–320.
- Ip Y.K. & Krisnaveni P. (1991) Incorporation of strontium ($^{90}\text{Sr}^{2+}$) into the skeleton of the hermatypic coral *Galaxea fascicularis*. *Journal of Experimental Zoology* **258**, 273–276.
- Jensen P.R., Gibson R.A., Littler M.M. & Littler D.S. (1985) Photosynthesis and calcification in 4 deep-water *Halimeda*-spp chlorophyceae caulerpales. *Deep-Sea Research Part I – Oceanographic Research Papers* **32**, 451–464.
- Kühl M., Glud R.N., Plough H. & Ramsing N.B. (1996) Microenvironmental control of photosynthesis and photosynthesis coupled respiration in an epilithic cyanobacterial biofilm. *Journal of Phycology* **32**, 799–812.
- Larkum A.W.D. (1999) The cyanobacteria of coral reefs. *Bulletin de l'Institut Oceanographique (Monaco)* **0**, 149–167.
- Li Y.-H. & Gregory S. (1974) Diffusion of ions in sea water and deep-sea sediments. *Geochemica Cosmochemica Acta* **38**, 703–714.
- Loban C.S. & Harrison P.J. (1997) *Seaweed Ecology and Physiology*. Cambridge University Press, Cambridge.
- McConnaughey T.D. (1987) Biomineralization mechanisms. In *Origin, Evolution and Modern Aspects of Biomineralization in Plants and Animals* (eds R.E. Crick), pp. 57–73. Plenum Press, New York.
- McConnaughey T.D. (1991) Calcification in *Chara corallina*: CO_2 hydroxylation generates protons for bicarbonate assimilation. *Limnology and Oceanography* **36**, 619–628.
- McConnaughey T.D. & Falk R.H. (1991) Calcium proton exchange during algal calcification. *Biological Bulletin* **180**, 185–195.
- Marshall A.T. (1996) Calcification in hermatypic and ahermatypic corals. *Science* **271**, 637–639.
- Raven J.A., Evans M.C. & Korb R.E. (1999) The role of trace metals in photosynthetic electron transport in O_2 -evolving organisms. *Photosynthesis Research* **60**, 111–149.
- Reid R.J. & Smith F.A. (1992) Regulation of calcium influx in *Chara*: effects of potassium, pH, metabolic inhibition, and calcium channel blockers. *Plant Physiology* **100**, 637–643.
- Revsbech N.P. (1989) An oxygen microelectrode with a guard cathode. *Limnology and Oceanography* **55**, 1907–1910.
- Revsbech N.P. & Jorgensen B.B. (1983) Photosynthesis of benthic microflora measured with high spatial resolution by the oxygen microprofile method: capabilities and limitations of the method. *Limnology and Oceanography* **28**, 749–756.
- Shimazaki K., Iino M. & Zeiger E. (1986) Blue light-dependent proton extrusion by guard-cell protoplasts of *Vicia faba*. *Nature* **319**, 324–326.
- Stento N.A., Ryba N.G., Kiegle E.A. & Bisson M.A. (2000) Turgor regulation in the salt-tolerant alga *Chara longifolia*. *Plant, Cell and Environment* **23**, 629–637.
- Tambutte E., Allemand D., Bourge I., Gattuso J.P. & Jaubert J. (1995) An improved ^{45}Ca protocol for investigating physiological mechanisms in coral calcification. *Marine Biology* **122**, 453–459.

Received 24 March 2001; received in revised form 12 July 2001; accepted for publication 12 July 2001